EEG Channel Interpolation using Ellipsoid Geodesic Length

Hristos S. Courellis*†, John R. Iversen†, Howard Poizner‡, Gert Cauwenberghs*‡
Email: {hcourell, jiversen, hpoizner, gert}@ucsd.edu
*Bioengineering Department, † Swartz Center for Computational Neuroscience, ‡ Institute for Neural Computation
University of California - San Diego, La Jolla, CA, USA

Abstract— **EEG channel interpolation is of great significance when the EEG signal from a channel is very low quality or missing altogether. This is particularly critical for low density EEG arrays employed in several clinical and research applications because the missing channel represents a large portion of the underlying cortical activity and adversely affects further data analysis and, potentially, diagnosis. For the same reasons, it is also critical for dry EEG applications when a disrupting contact is present. We present an approach for reconstructing a missing or poor EEG signal by combining signals from neighboring electrodes according to their distance from the electrode corresponding to the reconstructed signal. We used EEG data recorded from humans performing a cognitive task, omitted one channel at a time (to assess any spatial dependencies of our proposed approach), and reconstructed the omitted signal from the rest of the signals. Signals were reconstructed using Euclidean distance, great circle distance, and ellipsoid geodesic length and compared to reference (omitted) signals by means of inspection and normalized mean square error. Pilot results indicated that the ellipsoid geodesic length gave the best signal reconstruction as it provided event related potential and scalp map estimates closest to the reference and the smallest average (across all omitted channels) normalized mean square error (NMSE) values.**

Keywords—***EEG; Channel; Interpolation; Ellipsoid; Geodesic; Brain***

I. Introduction

EEG electrode arrays often used in both research and clinical applications are low density (typically 32 electrodes or fewer) and may be missing or having low quality data from a single position in the array, due to a faulty electrode or high impedance at that position, for example. The missing channel problem is notorious in the case of dry EEG as a temporarily (due to motion) or steadily (due to the presence of hair) disrupting contact [1]. As a result a sizeable region of the test subject's or patient's cortex suffers lack of coverage of [2], a critical deficiency in diagnosis and further data processing, since maximizing channel space information is critical for downstream analysis and source localization. Information about the mixing of electric fields and the geometric information from the position of the problematic electrode is lost and not available when computing current density on the cortical surface, a computational problem that is already ill-posed [3] even with full electrode coverage of the scalp.

Although it is not possible to fully recover the lost EEG signal, interpolation techniques exist that allow for reconstruction of the signal using information from the surrounding electrodes. Inverse distance weighting has been used to create a weighted average reconstructed signal, placing greater weight on the EEG signal from electrode locations proximal to the problematic electrode position and less weight on the EEG signal from locations distal to the problematic position [4]. This weighting is functionally consistent with the idea that channels closer to the missing position contain more information about the electric potential changes arising from cortical dipoles below the location of the missing electrode than channels farther away from the missing position. The naïve approach for computing pairwise distance between electrodes uses the Euclidean (L2) distance (EuD) metric ([5],[6]) and does not account for the geometry of the electrode array, which is wrapped around a subject's head, giving the array an ellipsoidal geometry. This geometry can be approximated either by a sphere or oblate ellipsoid and can use as distance metrics either the great-circle distance (GCD) or the ellipsoidal geodesic length (EGL) correspondingly to better represent the distance between electrode positions when interpolating missing signals.

In this paper, we interpolated channels by using EuD, GCD, and EGL to reconstruct missing EEG signals and compared each reconstructed signal to the reference (original) EEG signal by employing the normalized mean square error (NMSE). We employed multi-channel EEG data recorded from subjects performing a cognitive task [7], omitted one channel at a time, reconstructed the EEG signal for that channel, and compared the reconstructed EEG signals to the original signals of the omitted channels. The average (across all omitted channels) NMSE (ANMSE) and visual inspection of event-related potential (ERPs) and 2-D scalp maps associated to the cognitive task were employed to compare reconstructed signals to omitted signals. Cross-validation and parameter grid search were conducted using EEG data recorded from groups of human test subjects featuring electrode positions digitally registered after the electrode cap was wrapped around each subject's head.

II. Methodology

We performed reconstruction of omitted (missing) channel signals based on a weighed sum of signals from neighboring channels, using a weighing scheme that takes the inverse of the distance between the omitted channel and the corresponding neighboring channel into consideration. We evaluate the "goodness" of the reconstructed signals by means of the average normalized mean square error (ANMSE) which corresponds to the average over all channels of the normalized mean square error (NMSE) computed for each omitted channel estimate.

This work was supported by NSF ENG-1137279 (EFRI M3C)

A. Weighed Signal Reconstruction

The signal reconstruction approach for interpolating the missing (omitted) channels is based on employing weighted averages of the signals from neighboring channels [4]. The general expression for reconstructing the signal $\widehat{s_i}$ associated with channel-*i* from the signals ($s_j, j \neq i$) of neighboring channels can be expressed as the normalized weighed sum:

$$\widehat{s_i} = \frac{\sum_{j \neq i} w_{ij} * s_j}{\sum_{j \neq i} w_{ij}}, \quad w_{ij} = \frac{1}{d_{ij}^p} \qquad (1)$$

where w_{ij} corresponds to the weight on the contribution of the EEG signal (s_j) from position (channel)-*j,* expressed in terms of the inverse distance between positions *i* and *j* (d_{ij}^p) raised to a power p that is called the power parameter for the distance measure being considered.

B. Distance Dependent Weights

1)Euclidean Distance (EuD): The Euclidean distance between two electrode positions, electrode posistion *i* and *j*, is computed using the cartesian coordinate of each electorde position as follows:

$$d_{ij} = \sqrt{(X_i - X_j)^2 + (Y_i - Y_j)^2 + (Z_i - Z_j)^2} \qquad (2)$$

In this case, the weakness of Euclidean distance is that it does not accurately compute the distance between points on a curved surface. Since the skull of a human can be approximated with a sphere, the pairwise distance can be computed using Great-Circle Distance (GCD), the shortest circumferential distance between two points on the sphere.

2)Great-Circle Distance (GCD): This distance metric has been used in the past when interpolating weather patterns on the surface of the earth, thus allowing for direct mapping positions of latitude and longitude to the spherical coordinates used to represent electrode locations [4]. Due to the relatively small number of trigonometric functions it involves, the haversine formula was used to compute the GCD accurately over short distances and decrease the GCD's compute time for each pair of electrodes [8]. The haversine formula for computing GCD (d_{ij}) is shown below:

$$d_{ij} = 2 \sin^{-1} \sqrt{\sin^2(\frac{\varphi_i - \varphi_j}{2}) + \cos \varphi_i \cos \varphi_j \sin^2(\frac{\lambda_i - \lambda_j}{2})} \qquad (3)$$

The spherical coordinate positions of the electrodes are used to compute this distance, where $-2\pi \leq \lambda \leq 2\pi$ is the polar angle and $-\pi/2 \leq \varphi \leq \pi/2$ is the azimuthal angle. The radius of the circle is omitted since it has no effect on the final reconstructed sign.

3)Ellipsoid Geodesic Length (EGL): The skull was also approximated with an ellipsoid of revolution, and distances between electrodes were computed along the geodesics (shortest distances) that connect their associated points on the surface of the ellipsoid [9]. An ellipsoid of revolution was fit to the digitized electrode positions using a Least-Squares fitting approach and fixing the axes that incurred the lowest residual error between the ellipsoid surface and the electrode positions [9]. The major and minor axes of the fitted ellipsoid were then used to compute the geodesic distances using the Vincenty algorithm for solving the ellipsoid geodesic inverse problem, that is, computing the length of the geodesic given the latitude and longitude of the endpoints [10]. The algorithm is iterative, and fails to converge in cases where the electrode positions are near-antipolar. In these cases, the electrodes were simply omitted from the signal reconstruction for the position in question since, geometrically, the long distance between the electrodes would have placed a negligible weight on the antipolar position if it were included in the signal reconstruction. The equation for computing EGL (d_{ij}) is shown below:

$$d_{ij} = b\, A_{ij} \left(\sigma_{ij} - \Delta\sigma_{ij}\right) \qquad (4)$$

where b is the minor semi-axis of the ellipsoid, σ_{ij} is the angular distance between points *i* and *j*, and $A_{ij}$is a parameter associated with the Vincenty algorithm [8].

C. Power Parameter Estimation and ANMSE

The average normalized mean square error (ANMSE) was used as the measure to be minimized during the estimation of the power parameter. It generally reflects how well the channel interpolation performs in comparison to the reference. Small ANMSE values indicate better channel interpolation. For each omitted channel-*i*, the normalized mean square error (NMSE) was computed as:

$$NMSE(i) = \frac{\sum_t (s_{it} - \widehat{s_{it}})^2}{\sum_t {s_{it}}^2} \qquad (5)$$

where *t* represents the temporal index of the omitted EEG signal s_{it} and the reconstructed EEG signal $\widehat{s_{it}}$ associated with channel-*i*. The Mean Square Error (MSE was power normalized to prevent any individual electrode position whose signal exhibits very high power from dominating the MSE term, and, thus, misrepresenting the average performance of the distance metric at the current power parameter value in the parameter space.

Cross-validation was employed for determining the optimal power parameter for each distance metric via the computation of the ANMSE. This cross-validation process was rerun for every subject individually since, due to differences in head geometry and signal content, the optimal power parameter value varied across subjects. Cross validation was conducted separately for GCD to determine its optimal power parameter, which differed from the optimal Euclidean power parameter. Cross validation for the geodesic distances was conducted on a two dimensional parameter space, varying both the power parameter and the flattening of the ellipsoid--the flattening being used in the iterative portion of the Vincenty algorithm. The least-squares fit of the ellipsoid to the electrodes did not necessarily model the axes of the ellipsoid so that optimal signal reconstruction be achieved. To determine the flattening that allowed for optimal reconstruction, the minor axis of the ellipsoid was varied, and the error computed for every pair of power parameter and minor axis values in the parameter space. The optimal p value and minor axis length were selected as the point of the minimum in the two dimensional space.

III. RESULTS

EEG data recorded from a sixty four electrode array attached to the scalps of eleven individuals who participated in

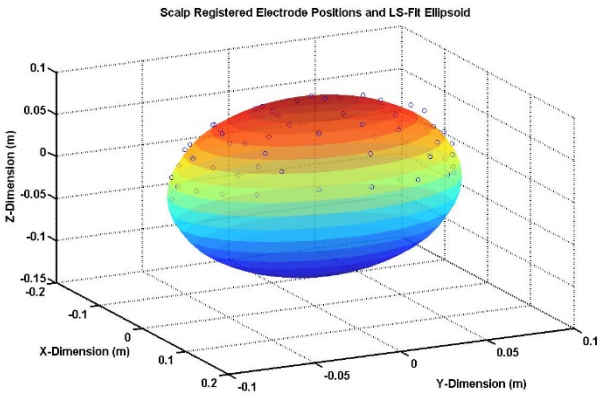

Fig. 1: Example of subject specific oblate ellipsoid fitted via least squares and digitally registered electrode positions (open circles).

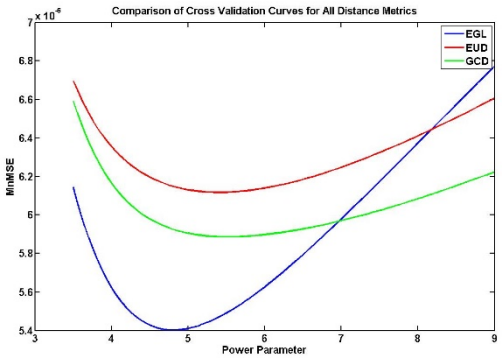

Fig. 2: Convergence profiles to the optimal power parameter for each distance measure: EuD-Euclidean Distance, GCD-great-circle distance, EGL-ellipsoid geodesic length. EGL gives the smallest ANMSE.

a cognitive visuomotor task (described in [7]) were used. The exact position of each electrode was digitally registered and a unique geometry was created for each test subject to which an oblate spheroid was independently fitted using least squares. The 64 electrodes in the array used for this study were enumerated based on their position. Figure 1 shows one such ellipsoid and the corresponding digitally registered electrodes.

The values for the power parameter to which the pairwise distance, serving as the basis for determining the weight placed on each neighboring signal, was raised were computed to be 5.4 for EuD, 5.65 for GCD, and 4.8, for EGL. Figure 2 shows the convergence profile to the optimal power parameter for each distance measure, which minimized the ANMSE. The smallest ANMSE of 8.01% was achieved when the EGL was employed for the power parameter value of 4.8. When EuD was used, the smallest ANMSE of 11.52% was achieved for the power parameter value of 5.4, while the smallest ANMSE of 10.37% was achieved, when GCD was used, for the power parameter value of 5.65. In the case of EGL, the convergence to the optimal power parameter included search for the smallest ANMSE over the power parameter and the ellipsoid flattening parameter space.

The fact that EGL provided the best weights for signal reconstruction was visually confirmed by means of reconstructed ERPs as they compare to the omitted (reference)

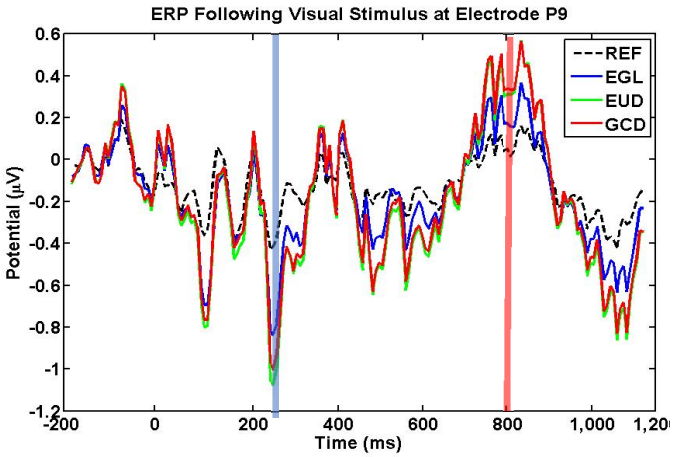

Fig. 3: Example of an ERP from an omitted channel (black dashed line) and the reconstructed ERPs for that channel using EuD (green trace), GCD (red trace) and EGL (blue trace). The EGL signal tracks the reference signal much better overall, especially during the latter part of the ERP.

ERP and reconstructed scalp maps of omitted electrodes (omitted one at a time) as they compare to reference scalp maps. Figure 3 presents an example of an ERP from an omitted channel (black dashed line) and the reconstructed ERPs for that channel using EuD (green trace), GCD (red trace) and EGL (blue trace). Although in some time intervals all four traces are close to one another, the EGL signal (blue trace) tracks the reference signal (dashed black trace) much better overall, especially during the latter part of the ERP. Scalp maps at two different time points one during the early phase (250 ms - blue vertical line) and another during the late phase (800 ms - red vertical line) of the ERP shown in figure 3 are depicted in figures 4 and 5 respectively. In both figures, panel (A) shows the scalp map estimate computed using EuD, panel (B) the scalp map estimate using GCD, panel (C) the scalp map estimate using EGL, and panel (D) the reference

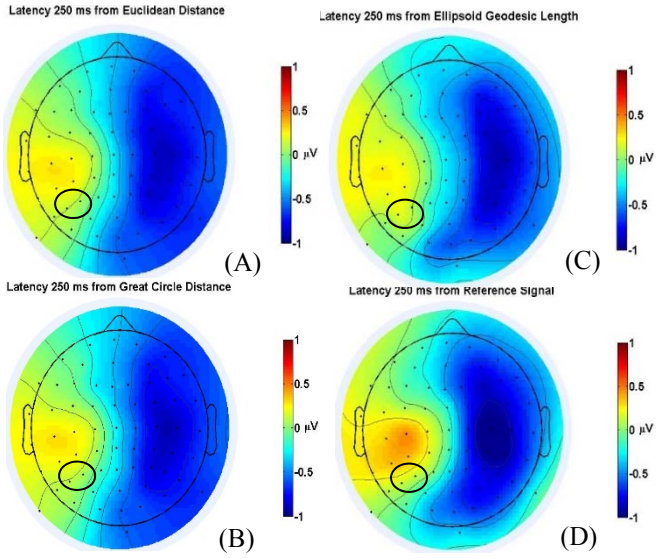

Fig. 4: Scalp maps corresponding to 250ms (blue vertical line) of the ERP shown in figure 4. Panels (A), (B), and (C) correspond to channel interpolation computed using EuD, GCD, and EGL based signal reconstruction, while panel (D) corresponds to the reference scalp map.

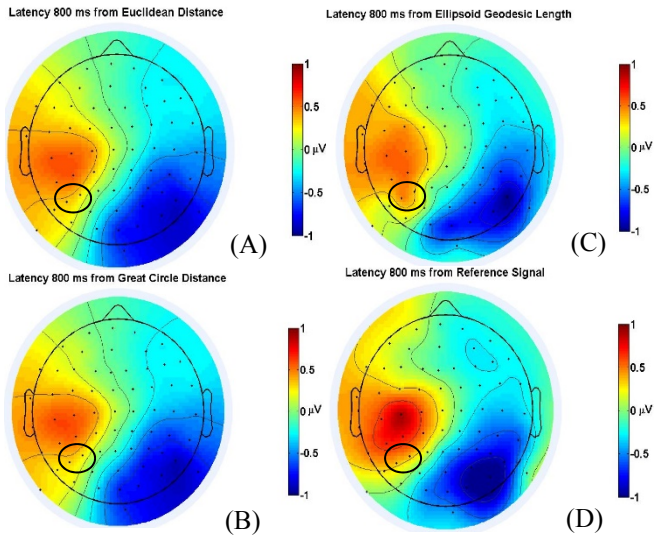

Fig. 5: Scalp maps corresponding to 800ms (blue vertical line) of the ERP shown in figure 4. Panels (A), (B), and (C) correspond to channel interpolation computed using EuD, GCD, and EGL based signal reconstruction, while panel (D) corresponds to the reference scalp map.

signal. At both time points, channel interpolation using reconstructed EEG signals based on EGL weighing performs best. Please, note that, in both cases, compared to the reference scalp map (panel D), EGL based channel interpolation (panel C) delineates negative activity (blue area on the scalp map) better than EuD or GCD scalp interpolation, providing sharper and more accurate (in terms of contour closure and density) transition to the positive area. It also better represents the increased activity of electrodes P3 and P5 (black circles).

IV. Discussion

EEG channel interpolation was conducted using three different distance metrics, and the performance of each metric was evaluated to determine which metric most accurately reconstructed missing EEG channel data. Reconstructing signals using EGL for the electrode pairwise distance yielded the lowest channel-average normalized mean squared error with respect to the reference signals.

The superior performance of EGL was also demonstrated by both the ERP computed for electrode position P9 (fig. 3) and the scalp maps presented in figures 4 and 5. In figure 4, over the course of the epoch, the reconstructed ERP based on EGL followed the reference waveform much more closely in amplitude than did the ERPs computed using the other two distance metrics, particularly during the positive voltage inflection about 800 ms and the negative voltage inflections about 250, 500, and 1000 ms. EGL also provided scalp maps more spatially consistent with the reference potential distribution on the surface of the scalp when compared to scalp maps computed using EuD and GCD. At the 250 ms scalp potential slice displayed across all electrodes, EGL captured the spatial distribution of the negative potential in the right hemisphere more accurately as it increased towards 0 μV around the edge of the electrode array, whereas both EUD and GCD overestimated the spread of the negative potential, showing it as extending to the very end of the array. In the positive potential region in the left hemisphere, EGL maintained signal power in electrodes P3 and P5 (encircled electrode locations in fig. 4), with the two exhibiting positive potential, as is the case with P3 and P5 in the reference signal. However, EUD and GCD showed these electrodes as having potential close to 0 μV (green), which is clearly not the activity present in the reference signal. These characteristics of EGL in comparison to EUD and GCD are maintained in the 800 ms scalp maps, where again, EGL much better approximated the negative potential region in the right hemisphere, without exhibiting the same overestimation of EUD and GCD, and maintaining the high positive power at positions P3 and P5 that EUD and GCD fail to support (encircled electrode locations in fig. 5). The contours of the positive EGL region also followed the reference signal more closely than the other two methods, showing high positive potentials in electrodes anterior to the left ear, whereas GCD and EUD dropped in potential magnitude at the front end of the ear. The findings for the pilot test subject suggest that EGL is a superior distance metric when used in a power augmented inverse distance weighting framework for EEG channel interpolation. A more extensive study should be conducted across multiple subjects to determine how consistent EGL is across various realistic head geometries. Nevertheless, EGL is a promising method in such clinical and scientific cases where missing EEG data must be interpolated with maximal spatial and temporal accuracy.

References

[1] T. R. Mullen et al., "Real-time neuroimaging and cognitive monitoring using wearable dry EEG," in IEEE Transactions on Biomedical Engineering, vol. 62, no. 11, pp. 2553-2567, Nov. 2015.

[2] G. H. Klem, H. O. Luders, H. H. Jasper, C. Elger, "The ten-twenty electrode system of the International Federation." *Recommendations for the Practice of Clinical Neurophys.: Guidelines of the International Federation of Clinical Physiology*, Elsiver Science B.V., 1999

[3] N. J. Trujillo-Barreto, E. Aubert-Vazquez, and P. A. Valdes-Sosa, "Bayesian model averaging in EEG/MEG imaging," Neuroimage, vol. 21, pp. 1300-1319, Nov 4 2003.

[4] S. M. Robeson, "Spherical Methods for Spatial Interpolation: Review and Evaluation," *Cartography and Geographic Information Systems*, vol. 24, pp. 3-20, Nov 1 1997

[5] F. Perrin, J. Pernier, O. Bertnard, M. H. Giard, J. F. Echallier, "Mapping of scalp potentials by surface spline interpolation," *Electroencepography and Clinical Neurophysiology*, vol. 66, pp. 75-81, Jan 1987

[6] M. S. Lemos, B. J. Fisch, "The weighted average reference montage," *Electroen. and Clinical Neurophys.,* vol. 79, pp. 361-370, Nov 1991

[7] J. R. Iversen, A. Ojeda, T. Mullen, M. Plank, J. Snider, G. Cauwenberghs*, et al.*, "Causal analysis of cortical networks involved in reaching to spatial targets " in *36th Annual International Conference of the IEEE Engineering in Medicine and Biology Society (EMBC)*, Chicago, Il., USA, 2014.

[8] R. W. Sinnott, "Virtues of the Haversine," *Sky and Telescope*, vol. 68, no. 2, pp. 159, Aug 1984

[9] A. Malyugina, K. Igudesman, D. Chickrin, "Least-squares fitting of a three-dimensional ellipsoid to noisy data," *Applied Mathematical Sciences*, vol. 8, no. 149, pp. 7409-7421, 2014

[10] T. Vincenty, "Direct and inverse solutions of geodesics on the ellipsoid with application of nested equations," *Survey Review*, vol. 22, no. 176, pp. 88-93, April 1975